ISTITUTO NAZIONALE DI GEOFISICA E VULCANOLOGIA

Site characterization report at the seismic station IV.VENL – Venezia Lido (VE)

Report di caratterizzazione di sito presso la stazione sismica IV.VENL – Venezia Lido (VE)

Working Group **Geology:** Paolo MANGANELLO, Sara LOVATI **Geophysics**: Rodolfo PUGLIA, Giulio BRUNELLI, Alessio LORENZETTI, Sara LOVATI, Paolo MANGANELLO, Marco MASSA	Date: December 2021
Subject: **Final report illustrating the site characterization for seismic station IV.VENL**	

Convenzione DPC-INGV 2019-21, All. B2 - WP1, Task 2: “Caratterizzazione siti accelerometrici” (Coord.: G. Cultrera, F. Pacor)
Cite as: Working group INGV "Agreement DPC-INGV 2019-21, All. B2- WP1, Task 2” (2021). Site characterization report at the seismic station *IV.VENL – Venezia Lido (VE).* http://hdl.handle.net/2122/15102

INDEX

INTRODUCTION

In this report we present the geological setting and the geophysical measurements and results obtained in the framework of the 2019-2021 agreement between INGV and DPC, called *Allegato B2: Obiettivo 1 - TASK 2: Caratterizzazione siti accelerometrici (Responsabili: G. Cultrera, F. Pacor)* for the site characterization of station IV.VENL (Venezia Lido).

Location and coordinates are reported in Table 1.

Table 1

CODE	NAME	LAT [°]	LON [°]	ELEVATION [m]
IV.VENL	Venezia Lido	45.41670 *	12.37650 *	4 **
ADDRESS	Public playground of Lungomare Gabriele D'Annunzio, 30126 Lido Venezia (VE), Italy			

* Coordinates from ITACA (Nov. 2021) ** Elevation from CTR 10k Regione del Veneto

A. Geological setting

A1. TOPOGRAPHIC AND GEOLOGICAL INFORMATION

Topographic information related to the site are reported in Table 2. Table 3 summarizes all available geological maps from literature for geological analyses.

Table 2

Topography	Description	Topography Class	Morphology Class
	Flat surfaces, isolated slopes and reliefs with slope i ≤ 15°	T1	Plain (P)

Table 3

Geological map	Source	Scale
IV.VENL	Geological Map of Italy (CARG Project) - sheet 128 (Venezia)	1:50.000

In Table 4 Geological, Lithological and Lithotechnical Units (according to Seismic Microzonation classification; Technical Commission SM, 2015) are described and are concerned to maps of following chapters. The term "original" means the result comes from a preexisting cartography (Table 3); the term "deduced" means the result comes from an interpretation of a preexisting cartography according to the nomenclature of corresponding cartography.

Table 4

GEOLOGICAL UNITS		**LITHOLOGICAL UNITS**		**LITHOTECHNICAL UNITS**	
Geological Map of Italy 1:50.000 (CARG Project) – sheet 128 (Venezia) *original*		Amanti *et al.* (2008) *deduced*		(MZS) *deduced*	
code	**description**	**code**	**description**	**code**	**description**
POI_{10}-s	Torcello Unit – littoral beach	B1	Sand, silt	SM sp	Sand-silt mixture
POI_{10}-l	Torcello Unit – littoral lagoon	B1-B2	Sand, silt, clay	ML pl	Fine sands, silts

A2. GEOLOGICAL MAP

In Figure 1 Geological Map is reported in a 1 $km \times 1$ km square around the station.

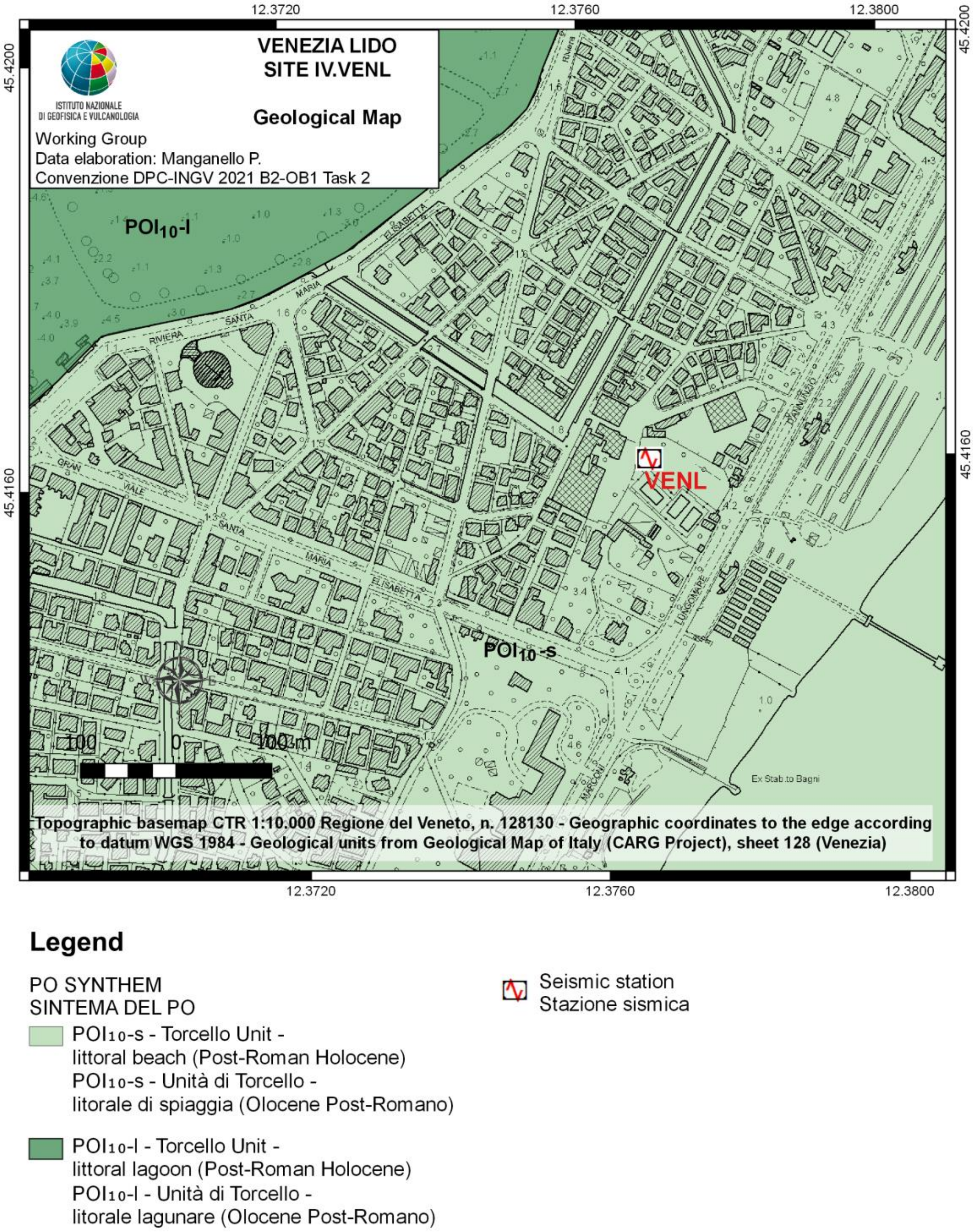

Figure 1: Geological map of seismic station IV.VENL. Scale 1:5.000. Geological units come from the Geological Map of Italy (CARG Project), sheet 128 (Venezia).

A3. LITHOLOGICAL MAP

In Figure 2 Lithological Map is reported in a 1 $km \times 1$ km square around the station.

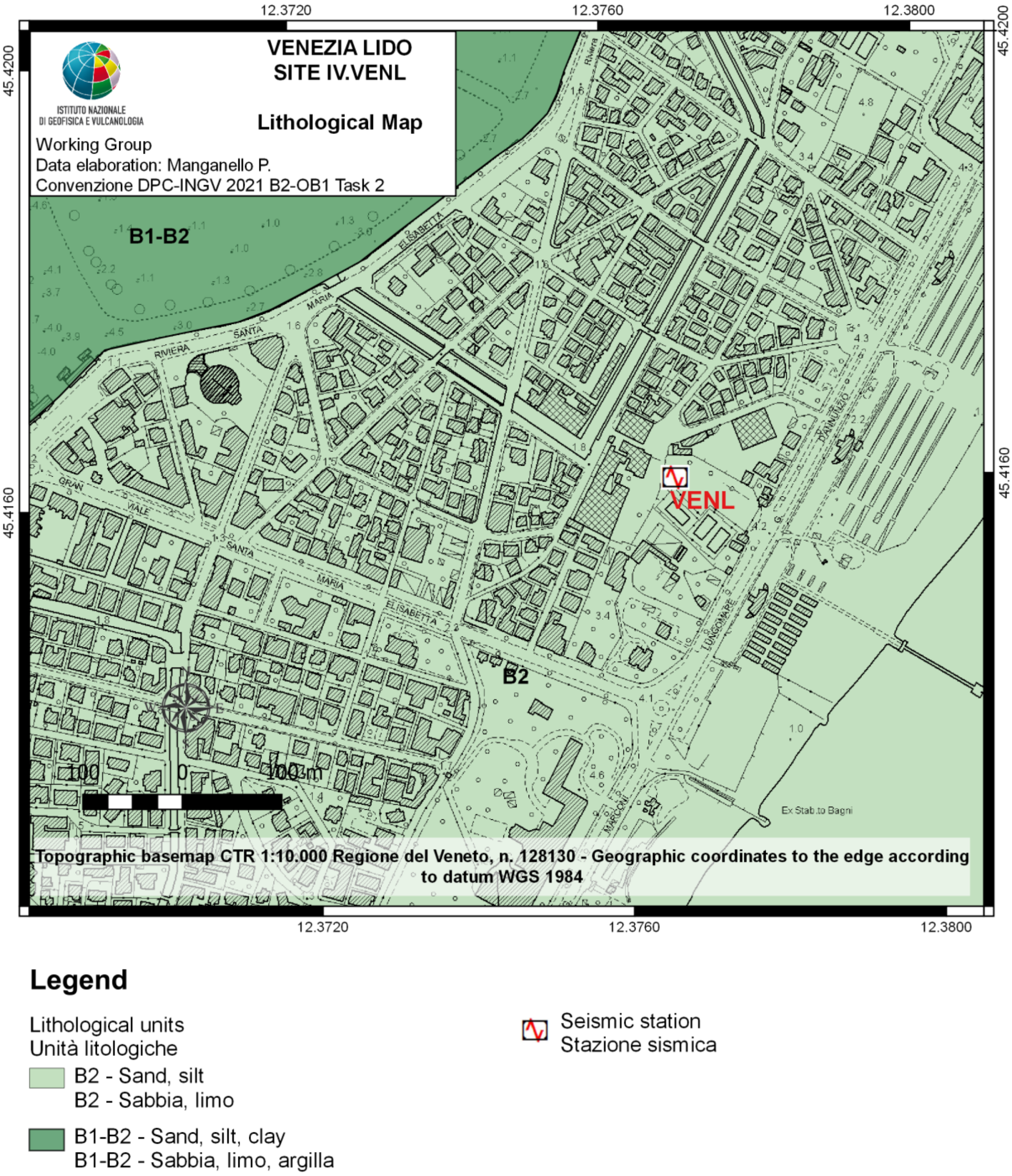

Figure 2: Lithological map of the seismic station IV.VENL. Scale 1:5.000. The codes of the lithological units are assigned according to the nomenclature of the Lithological map of Italy ISPRA 1:100.000 (Amanti *et al.*, 2008).

A4. LITHOTECHNICAL MAP

In Figure 3 Lithotechnical Map is reported in a 1 $km \times 1$ km square around the station.

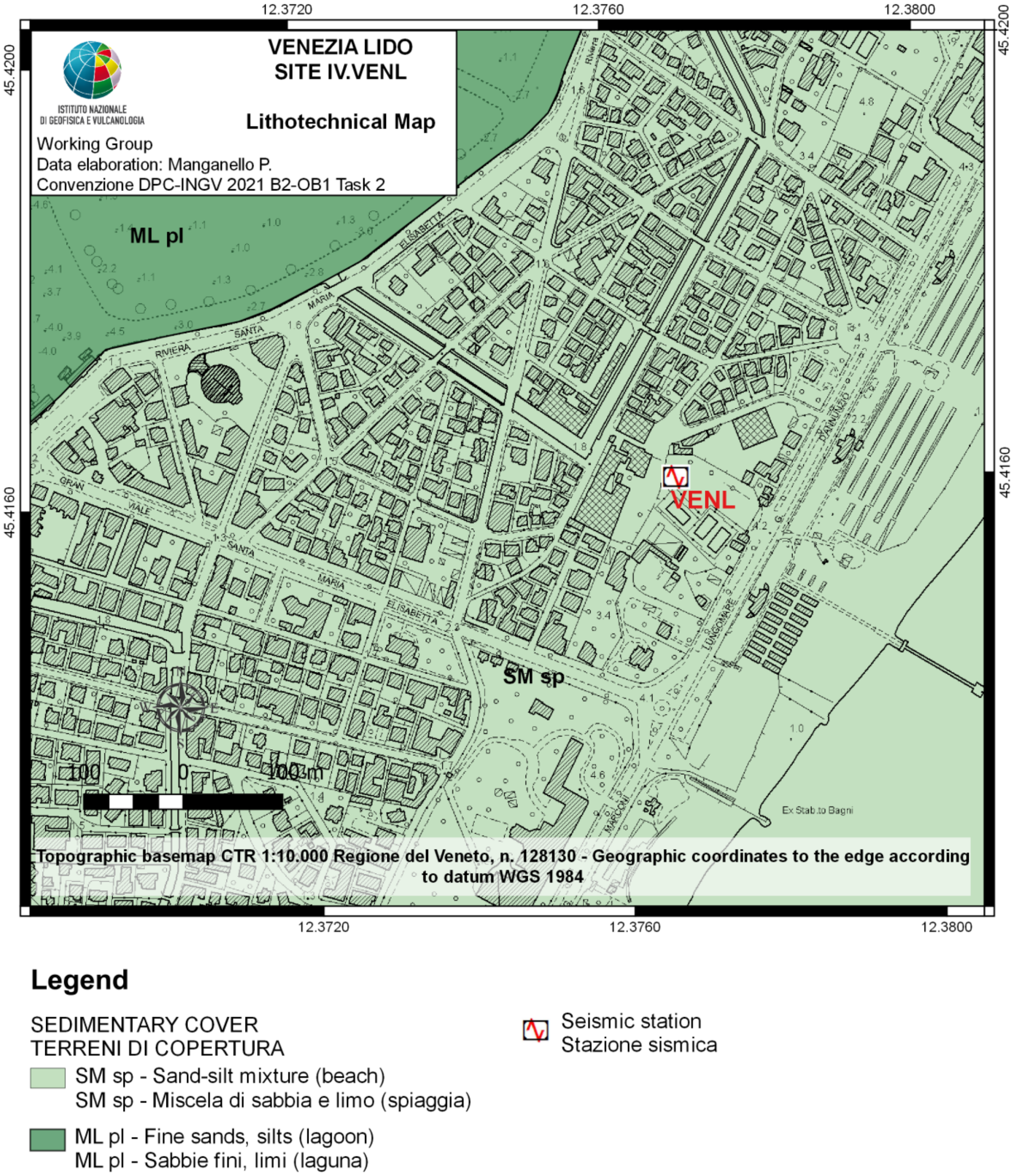

Figure 3: Lithotechnical map of the seismic station IV.VENL. Scale 1:5.000. The lithotechnical units are deduced according to the nomenclature of Seismic Microzonation (Technical Commission SM, 2015).

A5. SURVEY MAP

Figure 4 shows the Survey Map reporting both previous investigations and geophysical surveys conducted by INGV Working Group.

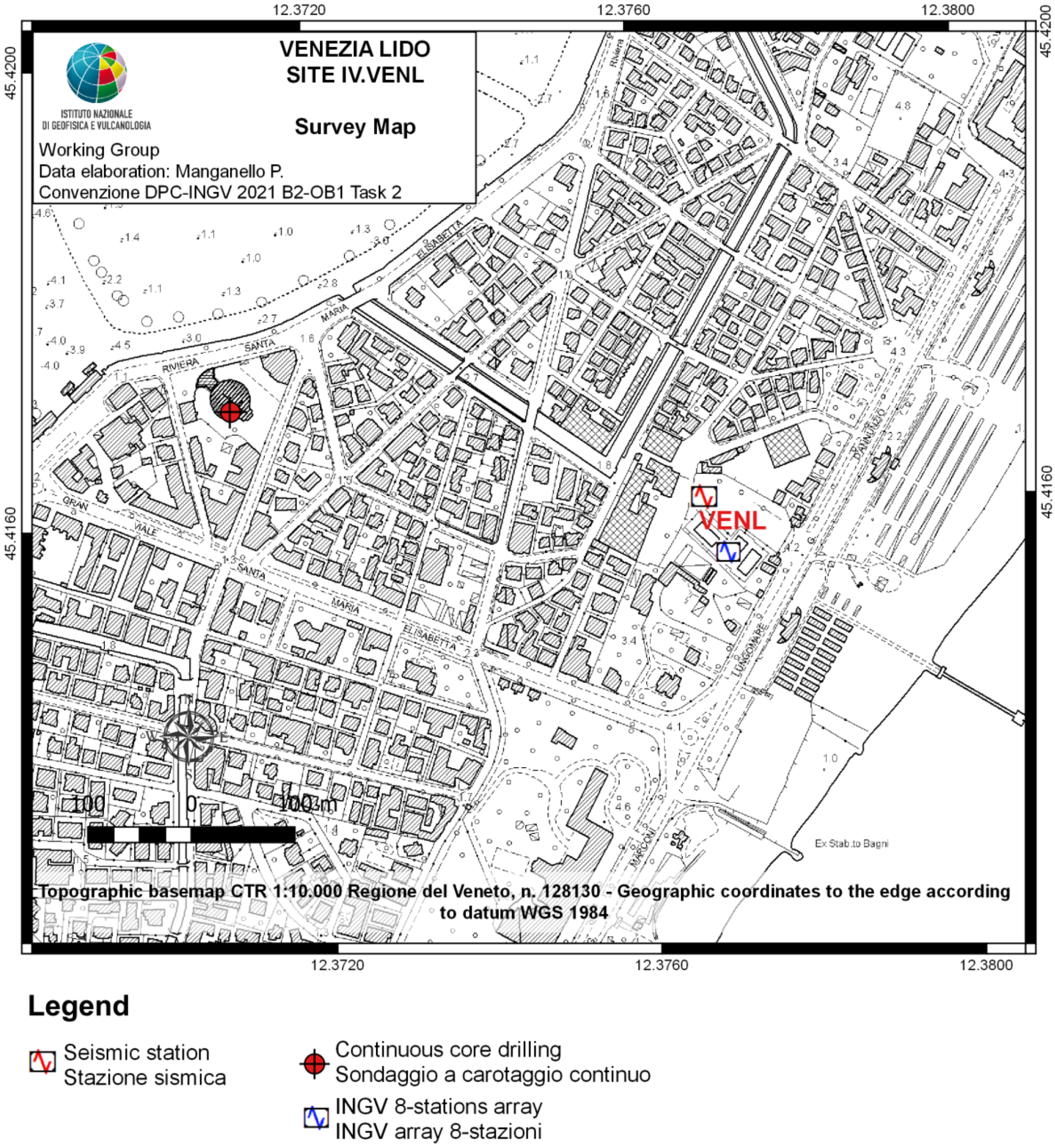

Figure 4: Map of the surveys in the surroundings of the station IV.VENL. Scale 1:5.000.

A6. GEOLOGICAL MODEL

6.1 General description

The seismic station IV.VENL is installed in the northern part of Lido littoral zone of Venice. The Venetian littoral zone extends for about 40 *km* and is bounded by the Brenta River to the South and the Sile River to the North. It is divided in four parts (Chioggia, Pellestrina, Lido and Cavallino) by three inlets which allow the exchange of the lagoon water with the water of Adriatic sea. The width of the four littoral zone strips changes from several kilometers at the two extremities close to the outflows of rivers to a few meters in the two central parts. The Venice area is situated in a complex foreland region located between the Southern Alps, the Northern Apennines and the Dinarides. After the deposition of the Mesozoic - early Cenozoic carbonates, the study area was characterized by the accumulation of Eocene to Miocene marly deposits. After the filling of the late Messinian incised valleys and the southward deposition of shallow-marine sediments in the Pliocene, a rapid drowning of the basin to bathyal depths linked to the development of the Apennine foredeep led to mostly turbidite sedimentation in the early Pleistocene. Deep-marine deposits pass upward into a NE-ward prograding sedimentary body representing a paleo Po-delta system that filled the Apennine foredeep, which is in turn overlain by an alternation between shallow-marine to continental sediments resulting from glacio-eustatic changes. The lagoon of Venice originated 6-7 kyr BP during the Flandrian transgression that caused the sea covered the Upper Adriatic Wurmian paleoplain (Tosi, 1994a; Tosi, 1994b; Carbognin *et al.*, 1995; Brambati *et al.*, 2003; Zecchin & Tosi, 2014).

6.2 Geological section

In the surroundings of IV.VENL seismic station, stratigraphic data are represented by a continuous core drilling (about 35 *m* deep). The WNW-ESE oriented geological section is reported and highlights the geological and structural setting of IV.VENL site. The trace with the location of the section is reported as a black line in the geological map (Fig. 5 upper left).

6.3 Subsoil model

The geological description reported from the surface to the bottom is described in the following part. A subsoil model is built up to a depth of 35 *m* on the basis of geological and stratigraphic information (Fig. 5 bottom). The stratigraphic succession starts with the Torcello Unit – littoral beach (POI_{10}-s), which belongs to the Po Synthem and has a thickness of about 5 *m*. This unit is characterized by sands, silty sands, silts and clayey/sandy silts of the Post-Roman Holocene. Below there is the Malamocco Unit – littoral beach (POI_9-s), which represents the lower part of the Po Synthem and reaches a depth of about 20 *m*. This unit is characterized by sands, silty sands, silts and clayey/sandy silts of the Pre-Roman Holocene.

At a depth of about 20 *m* there is presence of Mestre Supersynthem (MT), which is represented by alluvial deposits (sands, silts, clays) of the Upper Pleistocene.

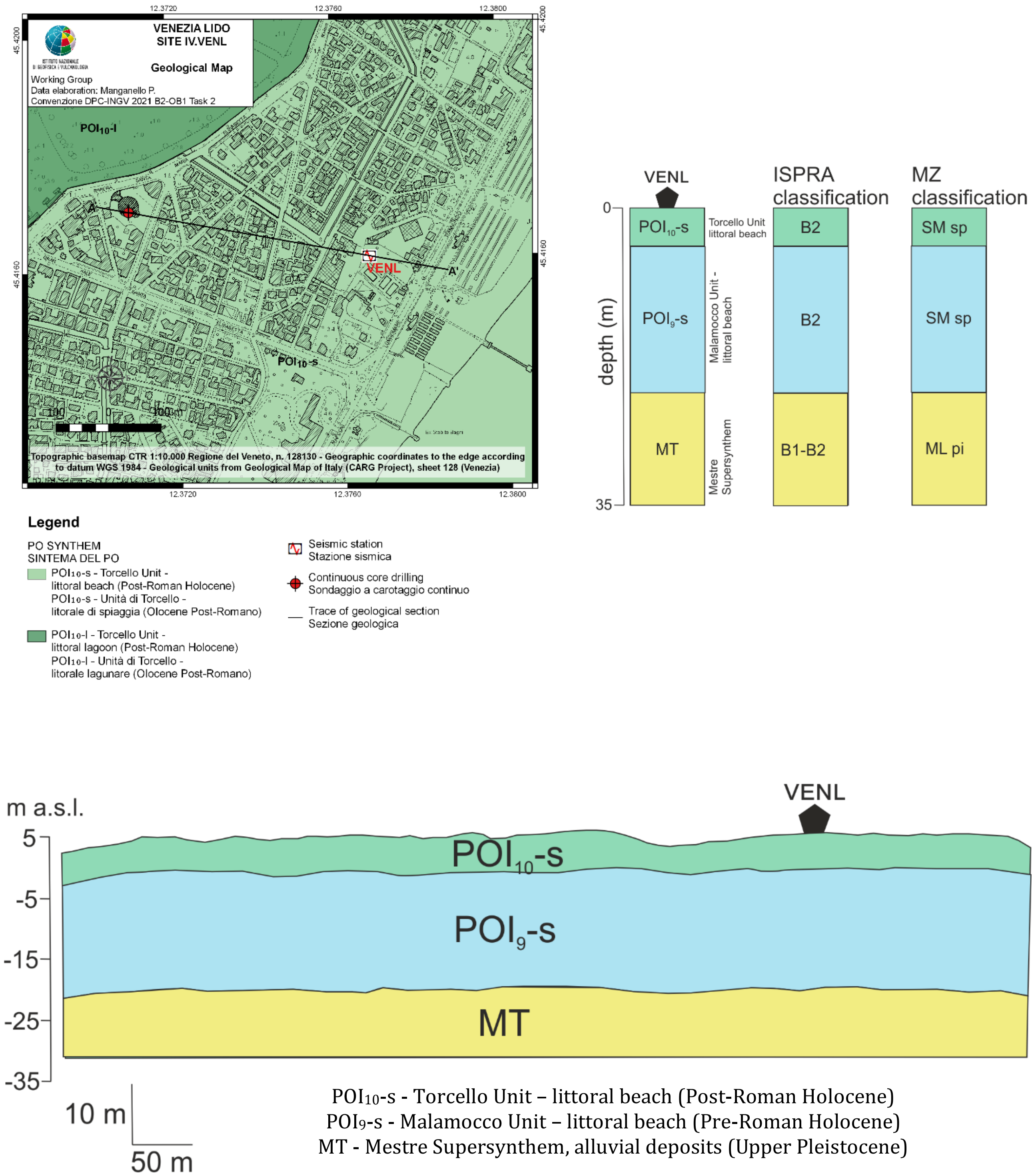

Figure 5: Upper left: Geological map of the study area where is installed IV.VENL seismic station. Upper right: Geological section. Bottom: Subsoil model for the site.

B. V_S profile

B1. GEOPHYSICAL INVESTIGATIONS

Geophysical measurements executed nearby the station VENL of the network IV (INGV, 2006) consist in ambient-vibration measurements in both single-station and 2D array configuration (Figure 6) that provide results in terms of resonance frequency of the soil deposits and in terms of dispersion curves of surface waves. These curves are inverted to obtain a shear-wave velocity (V_S) profile that, together with the geological study at section A, is suitable for assigning the soil class according to the current Italian seismic code (NTC18) and Eurocode (EC8). Figure 7 shows the location of the station IV.VENL (Latitude 45.4167, Longitude 12.3765 WGS84) installed in Venezia Lido (VE).

Seismic noise is acquired using 8 Reftek-130 24-bits recording systems equipped with short-period Lennartz LE-3D/5s sensors and GPS timing (Figure 7). The sampling rate is fixed to 200 *Hz*, while the gain is set as "high". Ambient noise recordings have a minimum duration of 1 hour. The array geometry (Figure 8) is chosen in order to have a good coverage of both azimuths and inter-station distances, the latter between the minimum (less than 10 *m*) and the maximum (about 30 *m*). These ranges allow the analysis of a range of wavelengths that guarantee sufficient shallow resolution (Okada, 2003) in order to estimate the $V_{S,30}$ and the site-class according to current building codes (i.e. NTC18 and EC8).

Figure 6: Map of the geophysical measurements performed at the IV.VENL site. The yellow place-markers indicate the geometry used for 2D array in passive configuration. The red triangle indicates the IV.VENL accelerometric station (image from Google Earth http://www.earth.google.com).

Figure 7: Left: IV.VENL accelerometric station installed in Venezia Lido (VE). Upper right: Single station ambient noise measurement. Bottom right: 2D passive ambient noise array installed close to the IV.VENL station.

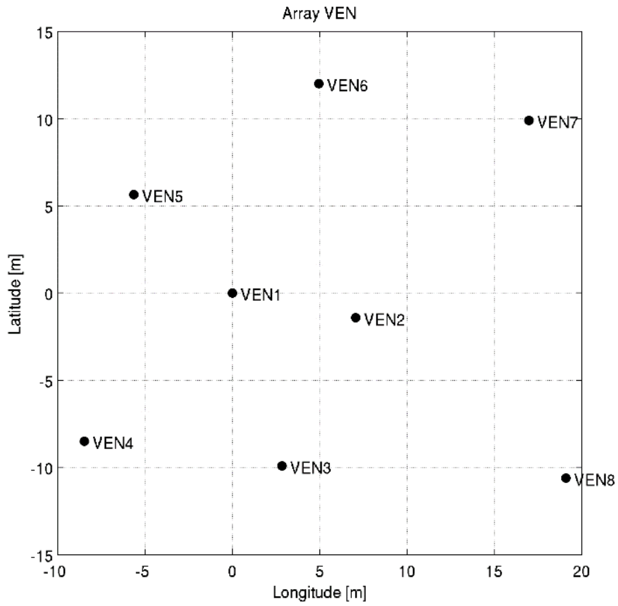

Figure 8: Array geometry.

The first step of the analysis consists in a visual inspection of the recordings at each station of the array. In particular, in order to identify malfunctioning and to select signal windows suitable for the surface wave analysis, the quality of the recording is evaluated analyzing the signal stationarity in the time domain, the relevant unfiltered Fourier spectra, and the H/V variation over time. Figures 9 and 10 provide graphical results about station VEN7.

It is common practice during surface wave investigation to verify the reliability of the one-dimensional site structure assumption (Aki, 1957; Okada, 2003). For this reason, we estimated the HVSR at each station of the array and the stability of HVSR among the array stations has been verified. Figure 11 depicts the HVSR assumed as representative for the array.

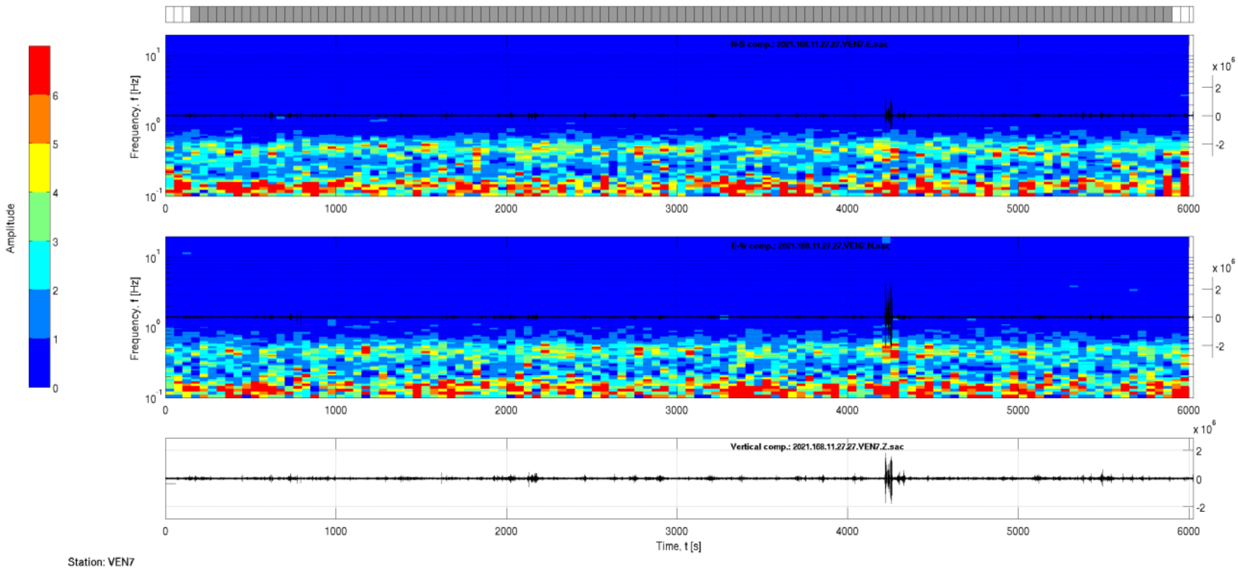

Figure 9: HVSR versus time (top and central panel for the NS and EW component, respectively) and corresponding time-histories.

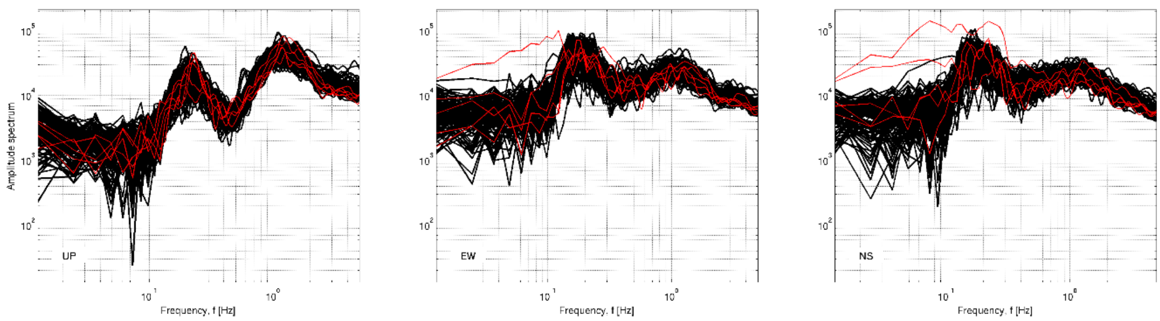

Figure 10: Fourier spectra for each noise window (left: Vertical, center: EW, right: NS). Red spectra are excluded from HVSR analysis.

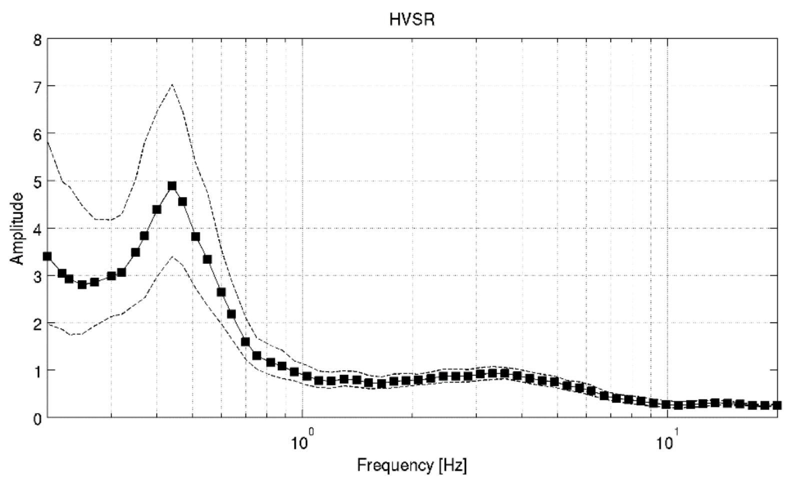

Figure 11: HVSR representative for the array. Dashed lines represent +/- one standard deviation.

The Rayleigh-wave dispersion curve is estimated by analyzing the vertical component of the recorded seismic noise. In particular, the Extended Spatial Auto-Correlation (ESAC; Ohori *et al.*, 2002; Okada, 2003) and the frequency-wavenumber (F-K; Lacoss *et al.*, 1969; Capon, 1969) methods are adopted. Further details about the combined use of ESAC and F-K approaches can be found in Parolai *et al.* (2006).

Both analyses use 60 synchronized signal windows of 60 *s* each, extracted from recordings within the UTC date-time interval 2021-06-17 11:55:00 – 2021-06-17 12:55:00, avoiding time periods affected by local disturbance.

The ESAC Rayleigh-wave dispersion curve is obtained by minimizing the root-mean-square (RMS) of the differences between experimental and theoretical Bessel functions (Figure 12). Values differing by more than two standard deviations from those estimated by the best fitting functions are automatically discarded (red circles in Figure 12) and the procedure is repeated iteratively. For this data set, data are also discarded whenever the inter-station distance is 2 times longer than the relevant wavelength. Figure 13 shows the Rayleigh-wave dispersion curve estimated using the ESAC approach.

The F-K analysis allows checking on the noise source distribution. One of the basic assumptions for the application of the ESAC method is indeed that the seismic noise wavefield is nearly isotropic. Figures 14 and 15 show results of the F-K analysis in terms of power density function for several frequencies using the Maximum Likelihood Method (MLM) and the Beam Forming (BF) respectively. Figure 16 shows the good agreement above 7 *Hz* between the Rayleigh wave dispersion curves estimated by both ESAC and F-K approaches. As expected, due to the array geometry, below this threshold the F-K analysis provides larger phase velocities.

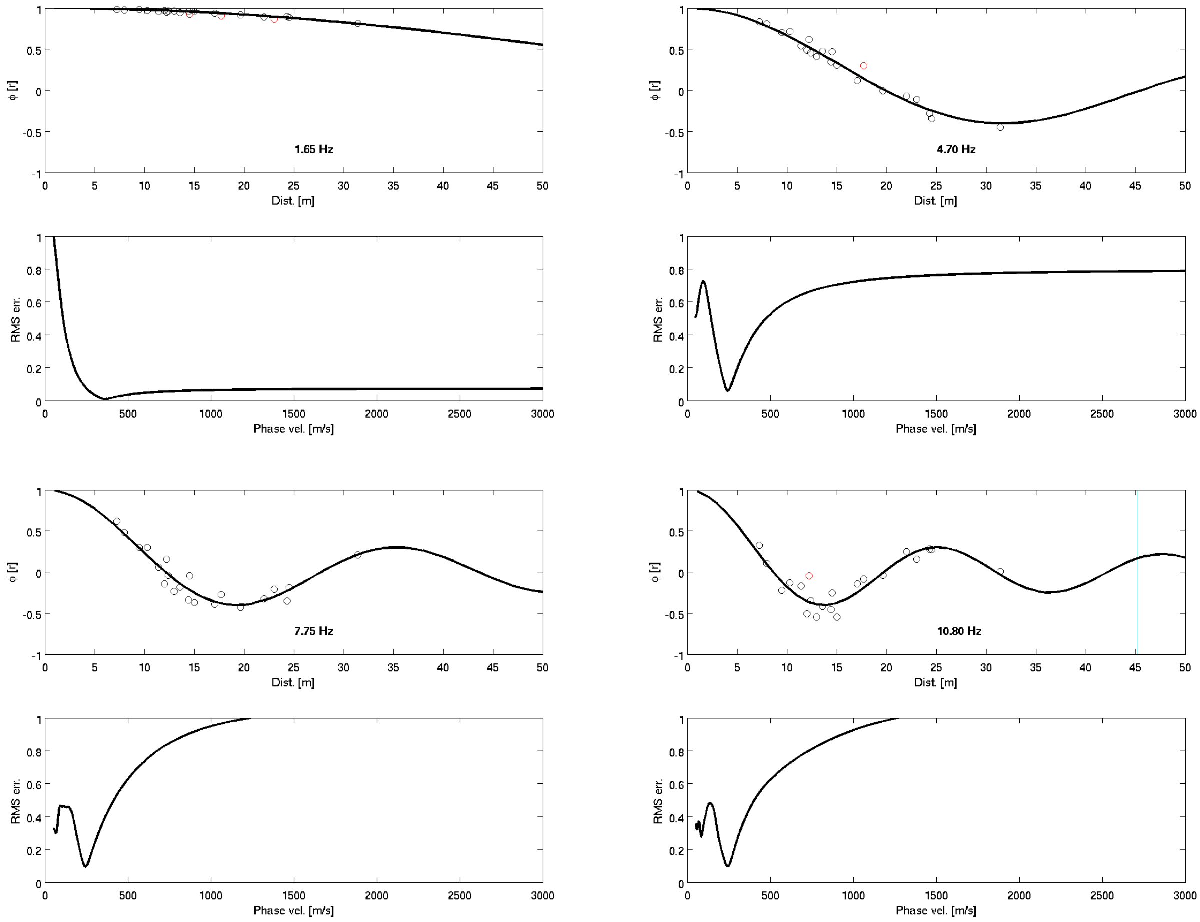

Figure 12: Experimental space-correlation function values versus distance (circles) for different frequencies. The red circles indicate values that are discarded. The black lines depict the estimated space-correlation function values for the phase velocity that furnishes the best fit to the data. The bottom panels show the relevant root-mean-square errors (RMS) versus phase velocity tested.

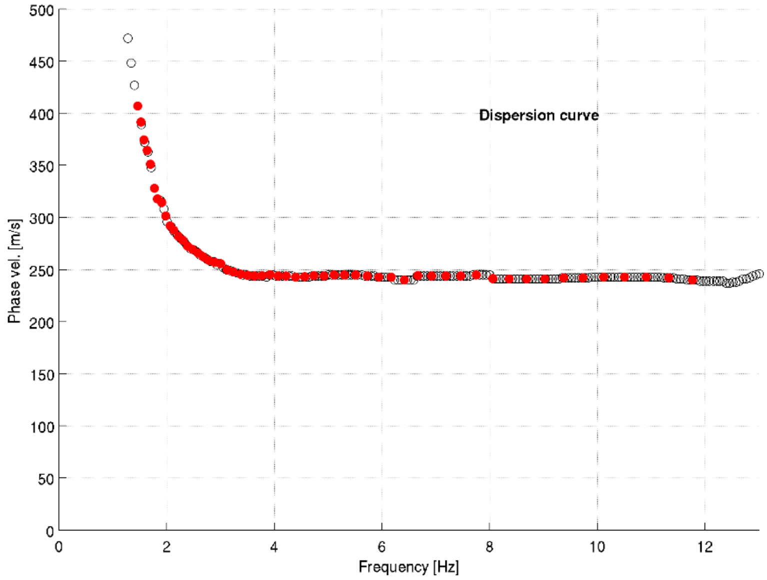

Figure 13: Rayleigh-wave dispersion curve from ESAC. Red-filled circles represent values potentially used for inversions.

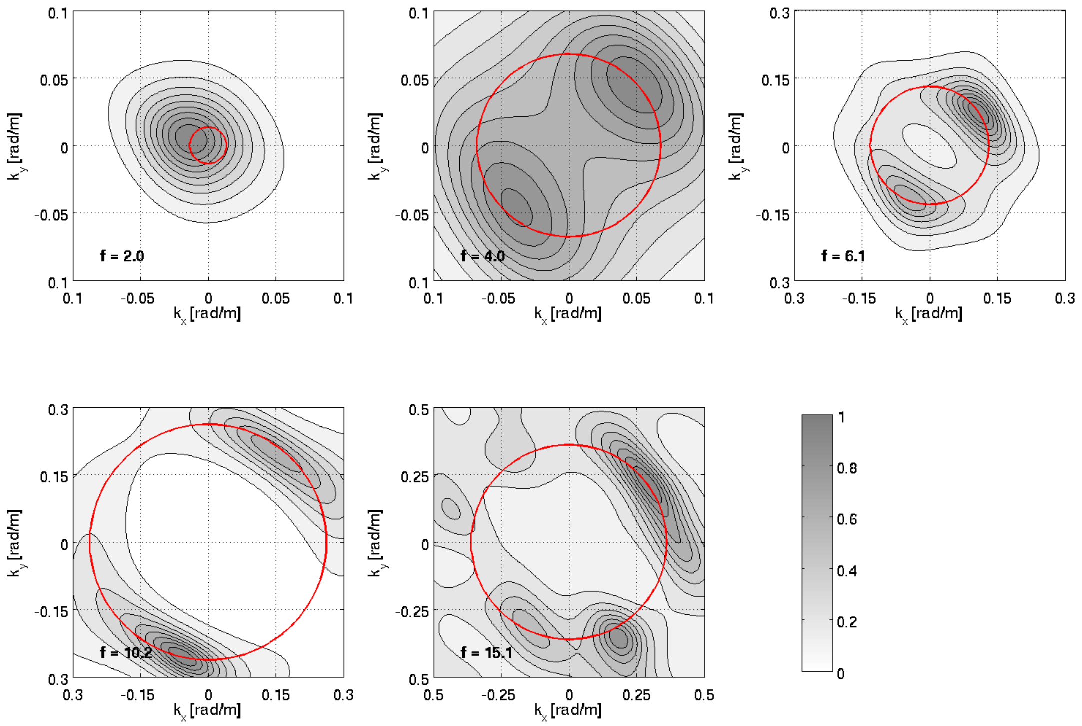

Figure 14: F-K power density function (Maximum-Likelihood Method) at selected frequencies.

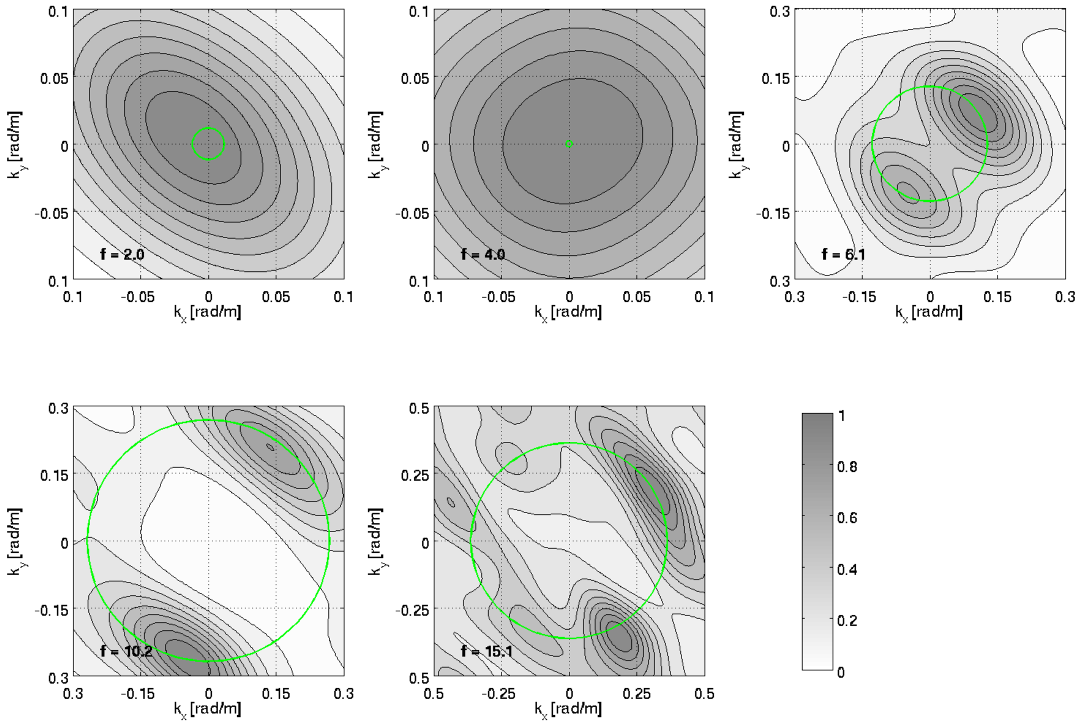

Figure 15: F-K power density function (Beam-Forming) at selected frequencies.

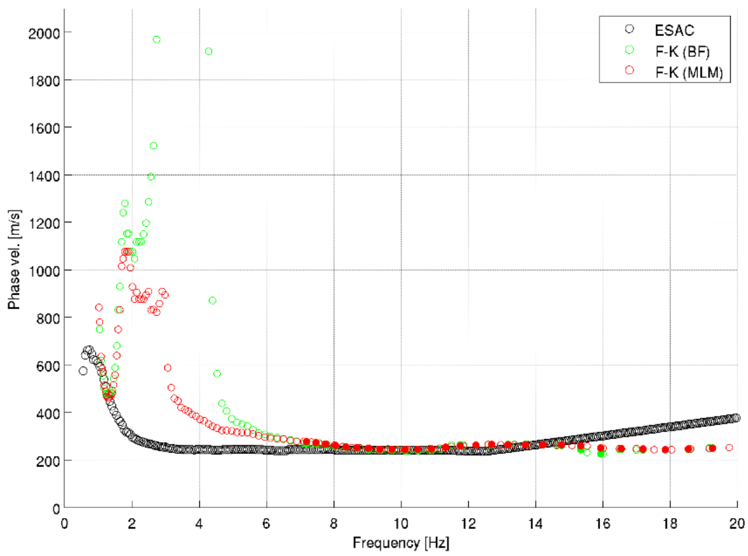

Figure 16: Comparison of experimental phase velocity estimated by the ESAC and the F-K (for both Beam-Forming and Maximum-Likelihood Method) methods. Filled circles represent values potentially used for inversions.

B2. SEISMIC VELOCITY MODEL

The non-linear inversions are performed using the software *joinv6* (Parolai *et al.*, 2005; Giustiniani *et al.*, 2020), which adopt a genetic algorithm (Yamanaka and Ishida, 1996). The forward modelling of Rayleigh wave phase velocities and HVSR curves is performed under the assumption of a vertically heterogeneous 1D Earth model using the modified Thomson-Haskell method proposed by Wang (1999) and following the suggestions of Arai and Tokimatsu (2004) and Tokimatsu *et al.* (1992). The modelling is not restricted to the fundamental mode, preserving the possibility that higher modes participate in simulating the observed dispersion and HVSR curves.

The experimental dispersion curve used as input for inversions is the one estimated from the ESAC analysis in the frequency interval 1.5-12 *Hz*. The experimental HVSR is used between about 0.2 and 1 *Hz*. In the left panel of Figure 17 tested models are shown in different colors according to their cost value: the more reliable model (minimum cost) is in white, the models lying inside the 10% range of the minimum cost are in black and the other tested models are shown in grey. In the right-central and right-bottom panels of Figure 17 agreement between experimental and theoretical (grey and open circles, respectively) Rayleigh-wave dispersion curves and HVSR are shown. The agreement is good and, considering the wavelengths related to the dispersion curve frequency range, the V_S profile between about 10-250 *m* is very well constrained. Table 5 reports the minimum-cost shear-wave velocity model.

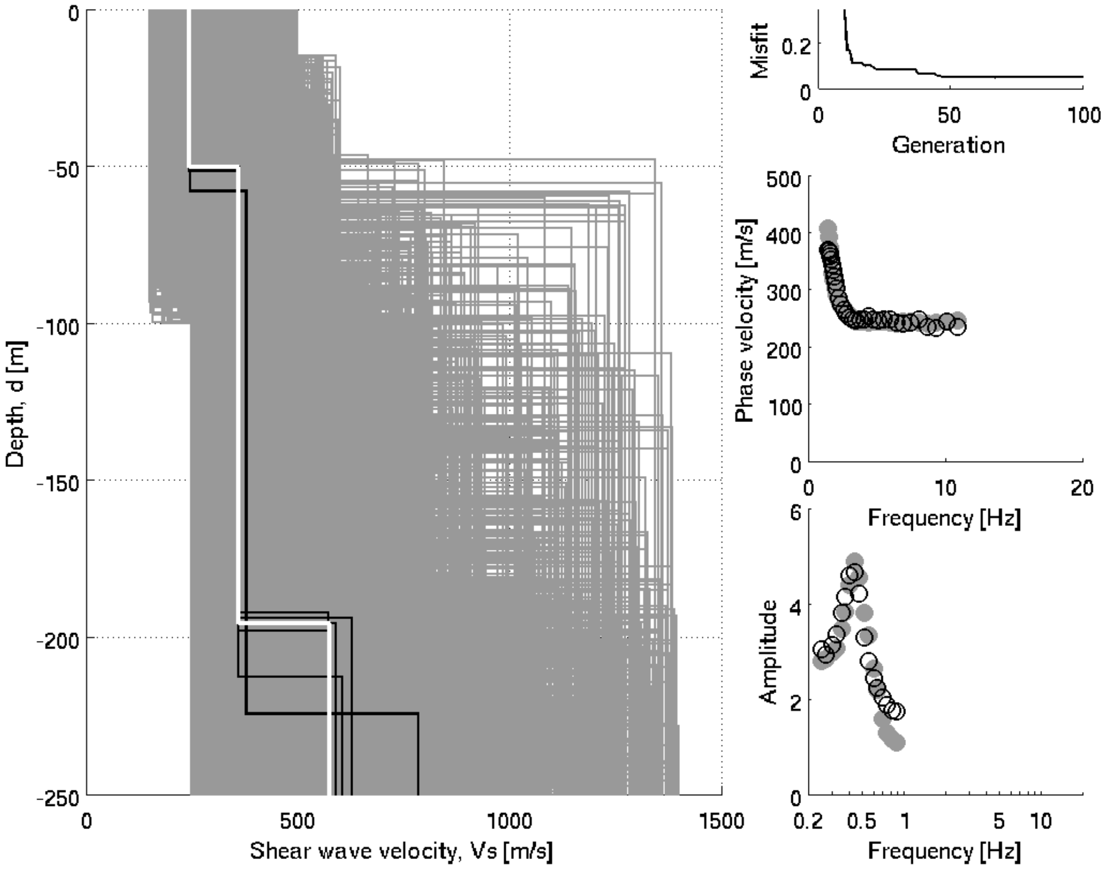

Figure 17: Shear-wave velocity models modeled during the inversion procedure (left panel): tested models (grey lines), the minimum cost model (white line) and models lying inside the minimum cost + 10% range (black lines); the generation values versus misfit (right-upper panel); the fitting of experimental data (grey circles) and empirical values relative to the minimum cost model (white circles) relevant to the dispersion curve (right-central panel) and to HVSR (right-bottom panel).

Table 5: Best-fit shear-wave velocity model

From [*m*]	To [*m*]	Thickness [*m*]	V_S [*m/s*]
0	50	50	245
50	196	146	360
196	-	-	577

B3. CONCLUSIONS

As evinced from results of geophysical investigations carried out by INGV Working Group, we can attribute to the littoral beach deposits of Torcello Unit and Malamocco Unit and to the alluvial deposits of Mestre Supersynthem a V_S value of around 245 *m/s*, compatible with EC8 class assigned at the site according to geological evidences.

According to the current Italian seismic code (NTC18), if the bedrock (V_S > 800 *m/s*) is more than 30 *m* in depth, the equivalent velocity ($V_{S,eq}$) is equal to the $V_{S,30}$. From Figure 17, the velocity of 800 *m/s* is reached for an unknown depth, well below the depth of 30 *m*.

Therefore, in this case, both $V_{S,eq}$ and $V_{S,30}$ are equal to 245 *m/s*. Of consequence, IV.VENL site is classified in the soil category C, for both the NTC18 and EC8 seismic codes (Table 6).

Table 6: $V_{S,eq}$,$V_{S,30}$ and soil classes

$V_{S,eq} = V_{S,30}$ [*m/s*]	Soil class (NTC18)	Soil class (EC8)
245	C	C

ACKNOWLEDGEMENTS

Authors wish to thank Stefano Parolai, Paolo Bernardi and Ilaria Dreossi (Istituto Nazionale di Oceanografia e di Geofisica Sperimentale - OGS), for providing us the software “joinv6”, which has been adopted as inversion procedure to estimate the shear-wave velocity model, and for the precious guide in its usage.

REFERENCES

Aki K. (1957). "Space and time spectra of stationary stochastic waves, with special reference to microtremors", Bulletin of the Earthquake Research Institute, 35, pp. 415–456.

Amanti M., Battaglini L., Campo V., Cipolloni C., Congi M. P., Conte G., Delogu D., Ventura R., Zonetti C. (2008). "The Lithological map of Italy at 1:100.000 scale: An example of re-use of an existing paper geological map", 33rd International Geological Conference, IEI02310L – 6-14th August, Oslo (Norway).

Arai H. and Tokimatsu K. (2004). "S-wave velocity profiling by inversion of microtremor H/V spectrum", Bulletin of the Seismological Society of America, 94, pp. 53–63.

Brambati A., Carbognin L., Quaia T., Teatini P., Tosi L. (2003). "The Lagoon of Venice: geological setting, evolution and land subsidence", Episodes, Vol. 26, no. 3, pp. 264-268.

Capon J. (1969). "High-resolution frequency-wavenumber spectrum analysis", Proceedings of the IEEE, 57, pp. 1408–1418.

Carbognin L., Marabini F., Tosi L. (1995). "Land subsidence and degradation of the Venice littoral zone, Italy", Land Subsidence (Proceedings of the Fifth International Symposium on Land Subsidence, The Hague, October 1995), IAHS Publ. no. 234, pp. 391-402.

EC8: European Committee for Standardization (2004). Eurocode 8: design of structures for earthquake resistance. P1: General rules, seismic actions and rules for buildings. Draft 6, Doc CEN/TC250/SC8/N335.

Foti S., Parolai S., Albarello D., *et al.* (2009). Deliverable 6: Application of surface wave methods for seismic site characterization. DPC-INGV S4 Project 2007-2009 (http://esse4.mi.ingv.it) – last accessed in June 2021 at http://esse4.mi.ingv.it/files/images/stories/deliverable_d6.pdf.

Foti S., Parolai S., Albarello D., et al. (2010). Deliverable 7: Application of surface wave methods for seismic site characterization of ITACA stations. DPC-INGV S4 Project 2007-2009 (http://esse4.mi.ingv.it) – last accessed in June 2021 at http://esse4.mi.ingv.it/files/images/stories/deliverable_d7.pdf.

Giustiniani M., Tinivella U., Parolai S., Donda F., Brancolini G., Volpi V. (2020). "Integrated Geophysical Analyses of Shallow-Water Seismic Imaging With Scholte Wave Inversion: The Northern Adriatic Sea Case Study", Frontiers in Earth Science, Vol. 8, p. 532. https://www.frontiersin.org/article/10.3389/feart.2020.587898 doi:10.3389/feart.2020.587898.

INGV Seismological Data Centre (2006). Rete Sismica Nazionale (RSN). Istituto Nazionale di Geofisica e Vulcanologia (INGV), Italy. https://doi.org/10.13127/SD/X0FXNH7QFY.

ISPRA – Geological Survey of Italy – Geological Map of Italy 1:50.000 (CARG Project) – https://www.isprambiente.gov.it/Media/carg/128_VENEZIA/Foglio.html.

Lacoss R.T., Kelly E.J. and Toksöz M.N. (1969). "Estimation of seismic noise structure using arrays", Geophysics, 34, pp. 21–38.

NTC18: Ministero delle Infrastrutture e dei Trasporti (2018). Aggiornamento delle Norme Tecniche per le Costruzioni. Part 3.2.2: Categorie di sottosuolo e condizioni topografiche, Gazzetta Ufficiale n. 42 del 20 febbraio 2018 (in Italian).

Ohori M., Nobata A. and Wakamatsu K. (2002). "A comparison of ESAC and FK methods of estimating phase velocity using arbitrarily shaped microtremor analysis", Bulletin of the Seismological Society of America, 92, pp. 2323–2332.

Okada H. (2003). The Microtremor Survey Method. SEG

Parolai S., Picozzi M., Richwalski S.M. and Milkereit C. (2005). "Joint inversion of phase velocity dispersion and H/V ratio curves from seismic noise recordings using a genetic algorithm, considering higher modes", Geophysical Research Letters 32, L01303. doi:10.1029/2004GL021115.

Parolai S., Richwalski S.M., Milkereit C. and Fäh D. (2006). "S-wave velocity profile for earthquake engineering purposes for the Cologne area (Germany)", Bulletin of the Earthquake Research Institute, 4, pp. 65–94. doi:10.1007/s10518-005-5758-2.

Regione del Veneto – Il Geoportale dei dati Territoriali – https://idt2.regione.veneto.it.

Technical Commission SM, 2015 – Microzonazione sismica. Standard di rappresentazione e archiviazione informatica, Versione 4.0b (Commissione tecnica inter-istituzionale per la MS nominata con DPCM 21 aprile 2011).

Tokimatsu K., Tamura S. and Kojima H. (1992). "Effects of multiple modes on Rayleigh wave dispersion characteristics", Journal of Geotechnical Engineering, 118, pp. 1529–1543.

Tosi L. (1994a). "I sedimenti tardo-quaternari dell'area litorale veneziana: analisi delle caratteristiche fisico-meccaniche", Lavoro svolto nell'ambito del Progetto Sistema Lagunare Veneziano - Linea di Ricerca 2.7, Geologia Tecnica & Ambientale, 2, pp. 47-60.

Tosi L. (1994b). "L'evoluzione paleoambientale tardo-quaternaria del litorale veneziano nelle attuali conoscenze", Il Quaternario, 7 (2), pp. 589-596.

Wang R. (1999). "A simple orthonormalization method for stable and efficient computation of Green's functions", Bulletin of the Seismological Society of America, 89, pp. 733–741.

Yamanaka H. and Ishida H. (1996). "Application of generic algorithms to an inversion of surface-wave dispersion data", Bulletin of the Seismological Society of America, 86, pp. 436–444.

Zecchin M., Tosi L. (2014). "Multi-sourced depositional sequences in the Neogene to Quaternary succession of the Venice area (northern Italy)", Marine and Petroleum Geology, Vol. 56, pp. 1-15.

[1]This document is level 3 as defined in the "Principi della politica dei dati dell'INGV (D.P. n. 200 del 26.04.2016)"